International Journal of Control, Automation and Systems 15(1) (2016) 49-58
http://dx.doi.org/10.1007/s12555-014-0125-1
ISSN:1598-6446 eISSN:2005-4092
http://www.springer.com/12555

Design and Analysis of A Modular Learning Based Cross-Coupled Control Algorithm for Multi-Axis Precision Positioning Systems

Nurcan Gecer Ulu, Erva Ulu and Melih Cakmakci*

Abstract: Increasing demand for micro/nano-technology related equipment resulted in growing interest for precision positioning systems. In this paper a modular controller combining cross-coupled control and iterative learning control approaches to improve contour and tracking accuracy at the same time is presented. Instead of using the standard error estimation technique, a computationally efficient and modular contour error estimation technique is used. The new controller is more suitable for tracking arbitrary nonlinear contours and easier to implement to multi-axis systems. Stability and convergence analysis for the proposed controller is presented with the necessary conditions. Effectiveness of the control design is verified with simulations and experiments on a two-axis positioning system. The resulting positioning system achieves nanometer level contouring and tracking performance.

Keywords: Cross-coupled control, iterative learning, mechatronic modularity, nano-positioning.

1. INTRODUCTION

In recent years increasing demand for micro/nano technology related equipment resulted in growing interest for precision positioning systems. Multi-axis precision positioning is crucial for applications such as micro/nano-scale manufacturing and assembly, optical component alignment, scanning microscopy, nano-particle placement and cell /tissue engineering [1–3]. These applications generally require both high contouring and tracking performance making their design process challenging. In tracking control, the primary objective is moving a predetermined point on the system along a desired trajectory. Although almost all systems employ feedback control, considerable improvement in tracking accuracy can be achieved by addition of feedforward control to the algorithm. Several feedforward control approaches are developed in literature to improve tracking accuracy such as zero phase error tracking control (ZPETC) [4–6], feedforward friction compensation [7, 8] and iterative learning control (ILC) [9–11]. Performance of a ZPETC system is sensitive to variations in plant parameters and modeling errors since it is based on pole/zero and phase cancellations [4]. Friction compensation techniques generally incorporate a system identification process that should be repeated if system parameters change. In [9] researchers claim that specifying a detailed plant model for ILC via zero phase filtering is not necessary due to the principle of self-support [12]. Since stored control signals from previous runs reflect the plant characteristics, ILC can improve tracking performance of a system even the plant structure and nonlinearities are unknown [13]. However, for ILC approach to provide improvements, the system should be executing the same task repeatedly such as in the case of manufacturing and assembling applications. Generally, improving tracking accuracy of an individual axis also increases the contouring accuracy of a multi-axis positioning system. However, in some cases where the effect of sub-system dynamics and the friction effects are dominant decreasing the tracking error per axis may not decrease the contour error. It may even deteriorate the contouring performance as reported in [14, 15]. Hence, the control algorithm should be designed considering not only the tracking error but also the contour error in order to achieve high accuracy for both. Koren [16] proposed the cross-coupled control (CCC) structure that focuses on

Manuscript received March 22, 2014; revised August 22, 2014 and December 30, 2014; accepted Febrary 20, 2015. Recommended by Associate Editor Won-jong Kim under the direction of Editor Hyouk Ryeol Choi. This research is sponsored by *Scientific and Technical Research Council of Turkey (TUBITAK) through Project No: 110M251*. The authors would like to thank undergraduate students Oytun Ugurel and Ersun Sozen for their support during computer aided design and drafting of the positioning system. Authors would also like to thank Dr. Sinan Filiz for sharing his experience in precision positioning systems.

Nurcan Gecer Ulu and Erva Ulu are graduate students with the Department of Mechanical Engineering, Bilkent University, 06800 Ankara, Turkey (e-mails: ulu@bilkent.edu.tr; erva@bilkent.edu.tr). Melih Cakmakci is with with the Department of Mechanical Engineering, Bilkent University, 06800, Ankara, Turkey (e-mail: melihc@bilkent.edu.tr).

* Corresponding author.

eliminating the contour error rather than the tracking error in individual axis. This method is proven to reduce contour error significantly. Since the introduction of the CCC, it has been modified and combined with different control techniques. Some examples can be given as the observer-based CCC [17], cross-coupled model reference adaptive control [18], CCC with disturbance observer and ZPETC [6], CCC with friction compensation [8] and CCC with ILC [10, 19, 20].

Since CCC based control schemes use the contour error as the input, there is a need for calculating this error in real time. Contour error is defined as the distance between the actual position and the nearest position on the contour [21]. Contour error can be calculated easily for linear contours. However, calculation procedure is very complicated for nonlinear contours, especially during real-time operation. Some approximations have been used to calculate the nonlinear contour error in real-time systems. The most common method is using the circular contour assumption suggested by Koren *et al.* [14]. Yeh and Hsu [21] proposed another method that approximates the contour error as the vector from the actual position to the nearest point on the line that passes through the reference position tangentially. The latter approach has several advantages over the former such as computational efficiency, applicability for arbitrary contours and convenience for multi-axis implementation [21]. Iterative Learning Control improves the tracking performance of the single axis positioning systems. By using the ILC with cross coupled control the contouring performance of the system can also be improve further. The method presented here implements CCC and ILC using the contour error vector approach as briefly outlined in [22]. It is computationally more efficient for calculating coupling gains of arbitrary nonlinear contours, modular in terms of including more axis which makes it easier to implement on multi-axis systems. Moreover, the proposed method utilizes ILC with zero-phase filtering which is more practical and suitable for modular systems where having unaccounted modeling uncertainties lower the system performance and modularity. The combined CCC and ILC with ZPF method presented here is used to achieve nanometer level precision (contouring + tracking) applied to a real-time positioning system. The multi degree of freedom system using our method is modular in the sense that multiple identical stages can be assembled together to form positioning systems without changing the stage control algorithm (i.e., mechatronic modularity). The increased modularity of the system compared to similar solutions is important since it improves desired life cycle properties.

The rest of this paper is structured as follows: In Section 2, system configuration and axis controller used in this study is introduced. Then, in Section 3, the CCC and ILC via zero-phase filtering is explained and the combined method is described. In Section 4, the stability and convergence analysis of the new method is presented. Simulation and experimental results are discussed in Sections 5 and 6, respectively. Conclusions and future work is presented in Section 7.

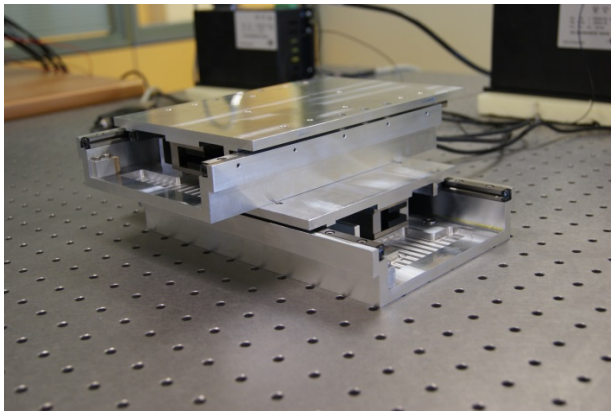

Fig. 1. Two-axis positioning system with identical stages.

2. SYSTEM SETUP AND AXIS CONTROL

The two-axis positioning system used in our studies is constructed by assembling two modular single-axis stages perpendicularly as shown in Fig. 1. This stage system is modular in the sense that multiple identical stages can be assembled together to form positioning systems without changing the stage control algorithm (i.e., mechatronic modularity). Modularity is important since it improves desired life-cycle properties such as maintainability, upgradability, diagnosability of a system. Interactions between module dynamics lower the modularity of the overall system lowering these desired properties. It is important to develop a controller modular in structure that is suitable for not only biaxial systems but also any multi-axis system.

The modular single-axis stage used in this study composed of a stationary base and a moving slider. These parts are connected to each other with cross-roller linear bearings. The stage is actuated by a brushless permanent magnet linear motor (PMLM) and the position feedback is received from an incremental linear encoder. The linear encoder has $1\mu m$ off-the-shelf resolution. However for our system, the encoder resolution is increased to $25nm$ using an interpolation technique discussed in [23]. Closed loop configuration of the single-axis stage is given in Fig. 2. A PC-based controller platform gives the positioning input to the system and runs the control algorithm in real-time. The control signal is sent to the amplifier by an analog output card in the controller. The position feedback is taken from the encoder by the data acquisition system and fed to the controller.

A simple diagram of the single-axis stage is given in

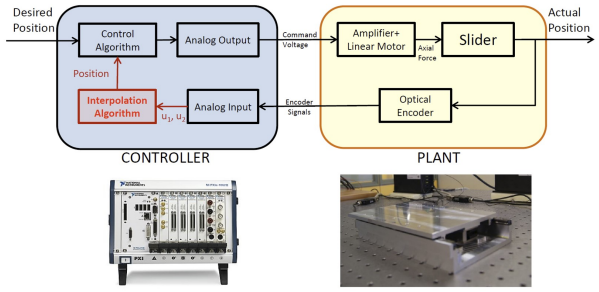

Fig. 2. Closed loop control setup of the single-axis system.

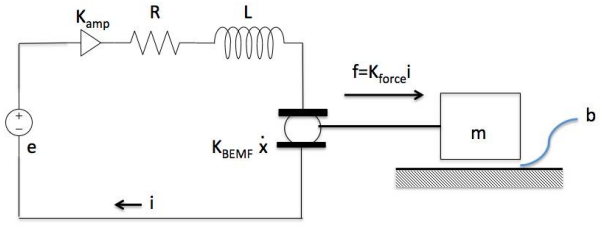

Fig. 3. Dynamic model of a single-axis system.

Fig. 3 where R is the linear motor resistance, L is the linear motor inductance, K_{BEMF} is the back electromotive force constant, K_{force} is the force constant, m is the sliding mass, b is the viscous friction, e_m is the linear motor input voltage, K_{amp} is the amplifier gain and i is the linear motor current. By applying the Kirchoff's Voltage Law and Newton's Second Law for the system given in Fig. 3 the system dynamic equations given in (1) and (2) respectively is obtained:

$$e_m K_{amp} - Ri - L\frac{di}{dt} - K_{BEMF}\dot{x} = 0, \tag{1}$$

$$m\ddot{x} + b\dot{x} - K_{force} i = 0. \tag{2}$$

Based on the equations given in (1) and (2) a transfer function between the stage displacement $X(s)$ to the applied voltage $E_m(s)$ is obtained as shown in (3).

$$P(s) = \frac{X(s)}{E_m(s)} = \frac{K_{amp}K_{force}}{s\left[Lms^2 + (Rm + bL)s + (Rb + K_{BEMF}K_{force})\right]} \tag{3}$$

In this dynamic model, ripple forces of the permanent magnet linear motor are neglected and linear bearings are modeled as a viscous friction component. For the transfer function of the plant shown in (3), viscous friction, and amplifier gain are unknown. A series of experiments are conducted to obtain a numerical expression for the transfer function between input voltage, e_m, and slider displacement, x. Based on (3), the transfer function of the single-axis slider system can be given in more general form as shown in (4) where G_{DC} is the DC gain of the slider system, ζ is the damping ratio, ω_n is the natural frequency, and τ is the time delay.

$$P(s) = \frac{X(s)}{E_m(s)} = \frac{G_{DC}\omega_n^2}{s(s^2 + 2\zeta\omega_n s + \omega_n^2)} e^{-s\tau} \tag{4}$$

In order to find the DC gain, G_{DC}, open loop velocity (i.e., $\dot{X}(s)$) step response of the plant can be used since there is no free integrator in the transfer function relating the velocity of slider to the applied voltage. In (5), the time domain response solution, $c(t)$, for an over-damped ($\zeta > 1$) unity gain second order system is given when the input function is the impulse function as reported in many sources such as [24].

$$c(t) = \frac{\omega_n}{2\sqrt{\zeta^2 - 1}} e^{-(\zeta - \sqrt{\zeta^2 - 1})\omega_n t} - \frac{\omega_n}{2\sqrt{\zeta^2 - 1}} e^{-(\zeta + \sqrt{\zeta^2 - 1})\omega_n t} \text{ for } t \geq 0 \tag{5}$$

The impulse response characteristics are examined through series of experiments. The peak (allowable) input value ($10V$) is applied for one time sample ($30ms$) emulating an impulse input while the response is recorded. By using this experimental data, and correlating the results with (5), system characteristic parameters ζ and ω_n are found as 1.1 and $150rad/s$ respectively. The time delay,τ, is also estimated as $0.015s$ by observing the closed loop step response for position loop and the controller output. A remedy such as a Smith Predictor can be used to overcome the negative effects of this delay. However since this delay is well below the control loop rate of our system ($30ms$), it is neglected during the controller design phase. Using the mathematical model derived from identification of the parameters in (4) a PID controller can be designed.

$$G_C(s) = K_p + K_i\frac{1}{s} + K_d s \tag{6}$$

In (6), the transfer function for such controller is given where K_p, K_i and K_d are the proportional, integral and derivative constants, respectively. The design objective is chosen such that the resulting closed loop transfer function for the slider speed simplifies to a first order transfer function with unity gain as shown in (7) where T_α is the desired time constant of the closed loop system response.

$$\frac{G_C(s)P(s)}{1 + G_C(s)P(s)} = \frac{1}{1 + sT_\alpha} \tag{7}$$

Using the PID controller parameters given in (8) the first order system given in (7) can be obtained.

$$K_P = \frac{2\zeta}{G_{DC}T_\alpha\omega_n}, \quad K_i = \frac{1}{G_{DC}T_\alpha}, \quad K_d = \frac{1}{G_{DC}T_\alpha\omega_n^2} \tag{8}$$

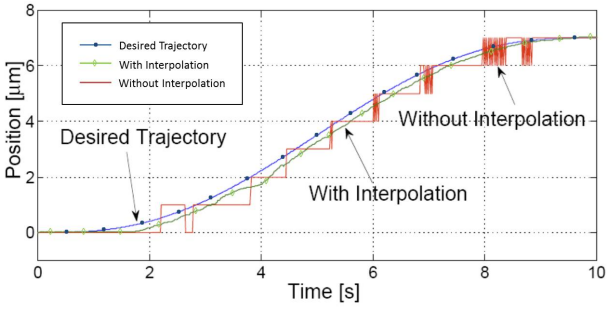

Fig. 4. Tracking performance of the single axis slider.

The positioning performance of the single axis slider system is evaluated with and without interpolation of the encoder signals. In Fig. 4, the tracking performance of the system for a reference input of *7mm* is given. In order to compare the tracking errors, the reference input is given as an *S*-curve. The improved tracking performance of the system is at sub-micrometer level. For the test 'without interpolation', RMS of the tracking error is calculated as *312.14nm*. When the encoder resolution is increased using the interpolation method, the same error is reduced to *121.53nm*.

3. MULTI-AXIS CONTROL DESIGN

In this section, a multi-axis control design method based on combining both CCC and ILC approaches is presented. Different contour error estimation techniques will also be discussed. The improved method which combines both approaches will be discussed at the last subsection.

3.1. Iterative learning control (ILC) via zero-phase filtering

ILC is a technique for improving the transient response of a system that performs the same task repeatedly under similar conditions. ILC can often be used to achieve perfect tracking, even when the dynamic model is uncertain or unknown and there is no information about the nonlinearities present in the system [13].

Using zero phase filtering is a practical and efficient implementation of ILC [9]. The block diagram for ILC with zero phase filtering for an individual axis is given in Fig. 5. In this diagram, u^i_{ff}, $u^i_{fb}$and y_i are the feedforward control signal, the feedback control signal and the system output at the i^{th} iteration, respectively. y_d is the desired system output which does not change between iterations and e is the tracking error. The feedforward control signal for the i^{th} iteration is calculated using the feedforward and feedback control signals of the previous iteration that are shown as u^{i-1}_{ff} and u^{i-1}_{fb}, respectively. The learning update

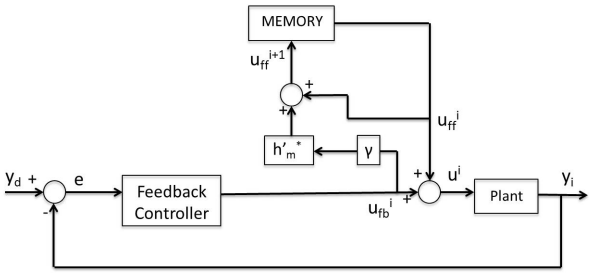

Fig. 5. Block diagram of ILC via zero-phase filtering.

law can be given as

$$u^i_{ff}(k) = u^{k-1}_{ff}(k) + \frac{\gamma}{2M+1}\sum_{j=-M}^{M} u^{i-1}_{fb}(k+j) \qquad (9)$$

where k is the time index, γ is the learning gain and M is the length index of zero phase filter. Detailed guidelines for the design of parameters g and M can be found in [9]. For the system given in this study, M is used as 11 and γ is taken as 0.2 giving the optimal learning performance. Although choosing suitable M and γ values is crucial for convergence, a suitable set of M and γ values can be used for different reference inputs. Once these values obtained, the same M and γ values are used in simulations and experiments for each axis.

3.2. Cross-coupled control (CCC)

Cross-coupled control is a special type of multi-input-multi-output (MIMO) control, which uses the contour error of the positioning system. The block diagram for a cross coupled controller is given in Fig. 6. In this block diagram, C_x and C_y are the coupling gains whereas ε, e_x, e_y are the contour error, x-axis tracking error and y-axis tracking error, respectively. The contour error, ε, is obtained using (10).

$$\varepsilon = -C_x e_x + C_y e_y \qquad (10)$$

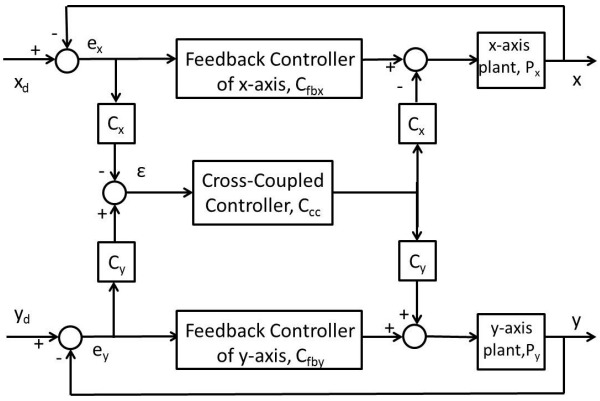

Fig. 6. Block diagram of the CCC system.

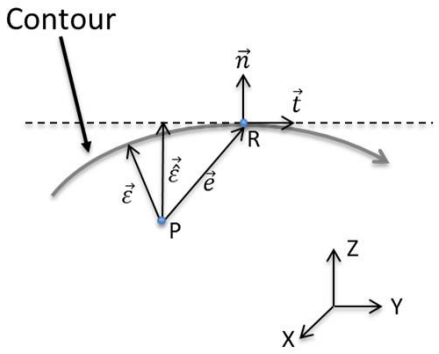

Fig. 7. Geometrical relations of contour error.

Although CCC is first introduced with constant gains [16], the term CCC is generally used for CCC with variable coupling gains (i.e. C_x and C_y) as proposed in [14]. For a nonlinear contour, calculation of these gains is very complicated and creates extra computational load in real-time systems. Therefore, some contour error approximations are needed to simplify the coupling gain computation. For this purpose, Koren [14] proposed the circular contour assumption. In this approach any arbitrary contour is separated into parts with radius of curvature ρ and these parts are approximated by circles.

The contour error vector approach can be explained using the geometrical relationships given in Fig. 7. In this figure, $\overrightarrow{t}$ and $\overrightarrow{n}$ are the normalized tangential and normal vectors respectively based on the actual position, P and the reference position, R. The contouring error, $\overrightarrow{\varepsilon}$, is defined as the vector from the actual position to the nearest point on the line that passes through the reference position tangentially in the direction of $\overrightarrow{t}$. This approach estimates contour error vector very closely when tracking error is small enough [21]. The estimated contour error, $\overrightarrow{\hat{\varepsilon}}$, is equal to $\langle \overrightarrow{e}, \overrightarrow{n} \rangle$ where $\overrightarrow{e}$ is the tracking error and $\langle ., . \rangle$ is the inner product operator. The contour error is calculated as $\left|\overrightarrow{\hat{\varepsilon}}\right| = \int_i C_i e_i$ $(i = \{x, y\})$ where C_i is coupling gain and e_i is the corresponding tracking error for each axis. By equating the two representations of estimated contour error vector, $\overrightarrow{\hat{\varepsilon}}$, cross coupling gains $(C_x,\ C_y)$ are found as $C_i = n_i (i = \{x, y\})$. In other words, cross coupling gains at a specific point on the contour are the elements of $\overrightarrow{n}$ of the contour at that point.

Although these two approaches for estimating contour error give similar results in terms of contouring accuracy, contour error vector method has several advantages over the circular contour assumption. An extensive study on the computational efficiency of the contour error vector approach over the circular contour approach is given in [21]. With the contour error approach, coupling gains can be computed easier for an arbitrary contour making implementation of this approach in multi-axis systems straightforward. The use of individual vector elements rather than a composite calculation using each axis information also improves the modularity of the resulting controller.

3.3. The combined (modular ILC+CCC) method

For most positioning applications, designing a controller with high tracking and contouring performance at the same time is desirable. The two-axis positioning system is designed such that two mechatronically modular (i.e., identical hardware and software) single-axis stages are assembled on top of each other as shown in Fig. 1. Although this paper focuses on simulation and real time control of two-axis system, control method developed is applicable to multi-axis systems with any number of axes. The use of ILC is important for the modularity since the method compensates for changes after the assembly. For example, when a stage is assembled on top of another, weight of the sliding mass changes for the bottom slider. Since there are only two design parameters in ILC via zero-phase filtering, the implementation is also simple. The contour error vector method is used with the CCC since it is computationally more efficient and axis modular in nature. For the system used in this study, optical encoder information is interpolated to achieve nanometer resolution using software algorithms. There is a trade-off between the resolution of the encoders and the computational effort in the control loop. Therefore, it is important to minimize computational effort in the control loop to maximize the encoder resolution.

A generalized block diagram of the proposed control algorithm is given in Fig. 8. Parameters of the figure are given in Table 1. The desired input trajectories are provided to the system as the $\boldsymbol{r}_d$ vector. Then, the axial tracking errors are found as the $\boldsymbol{e}$ vector and sent to the feedback controller $\boldsymbol{C}_{fb}$. Also, the contour error, $\boldsymbol{\varepsilon}$ is calculated multiplying the transpose of the coupling gain vector, $\boldsymbol{C}_T$, and the axial error vector. Contour error is sent to the cross-coupled controller, $\boldsymbol{C}_{cc}$, and the output is multiplied by coupling gain vector to find the cross coupled

Table 1. Parameters (NS is the number of samples)

Symbol	Description (Dimensions)
$\mathbf{r_d} = [x_d, y_d]^T$	desired input trajectory $(2xNS)$
$\mathbf{r} = [x, y]^T$	output trajectory $(2xNS)$
$\mathbf{e} = [e_x, e_y]^T$	axial tracking error $(2xNS)$
$\mathbf{e}_u = [eux, euy]^T$	uncoupled axial tracking error $(2xNS)$
$\mathbf{u^i} = [u_x^i, u_y^i]^T$	axial driving signal at i^{th} iteration $(2xNS)$
$\mathbf{u}_{ff}^i = [u_{ffx}^i, u_{ffy}^i]^T$	combined control signal $(2xNS)$
$\mathbf{C} = [C_x, C_y]^T$	coupling gains $(2x1)$
$\mathbf{C}_{fb} = diag\{C_{fbx}, C_{fby}\}$	feedback controller matrix $(2x2)$
$\mathbf{P} = diag\{P_x, P_y\}$	controlled plant $(2x2)$
C_{cc}	cross-coupled controller $(1x1)$
γ	learning gain
hl_{m*}	alg. averager for ILC
ε	contour error $(1xNS)$
ε_u	uncoupled contour error $(1xNS)$

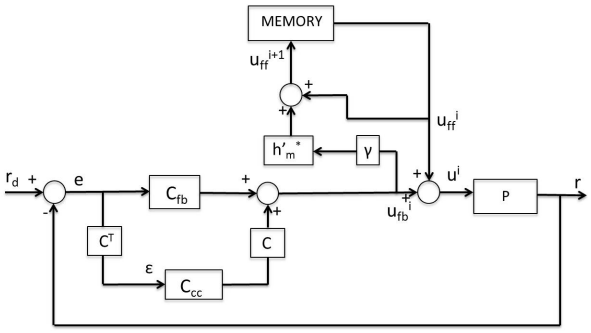

Fig. 8. Block diagram for the combined (ILC+CCC) control method.

control input for each axis. After adding the cross-coupled control signal to the feedback control signal, the combined signal, $\boldsymbol{u}_{fb}{}^{i}$,is send to the iterative learning controller to the filter, (h'_m) and stored to be used in the next iteration. The feed-forward control signal, $\boldsymbol{u}_{ff}{}^{i}$, is added to the combined signal and given to the plant. The expected benefits of the method described here is good tracking performance (due to ILC features) and good contouring performance (due to the application of CCC) with low computational effort which is applicable to systems with any number axis.

4. STABILITY AND CONVERGENCE ANALYSIS

Analyzing the stability and convergence of a new control method is important for safe implementation in real systems. The proposed control system consists of three parts: (1) The feedback controllers for each axis, (2) A cross-coupled controller for axis interactions and (3) Iterative learning controllers for each axis.

A stabilizing controller can be designed for each singleaxis slider using conventional control design methods. Then, a stable cross-coupled controller should be designed. For cross-coupled systems, stability can be analyzed through a term called contour error transfer function (CETF). The CETF is the relationship between a coupled and uncoupled system. Coupled system refers to a system controlled by a cross-coupled controller and uncoupled system refers to the same system only without the cross-coupled controller. Both coupled and uncoupled systems are considered without the ILC first. To derive the CETF, contour error should be derived without the CCC and with the CCC as ε_u and ε, respectively based on the system given in Fig. 6. The axial errors in the uncoupled system, eu, (i.e. $C_{cc} = 0$) is defined as

$$\begin{aligned} e_u &= r_d - r = r_d - PC_{fb}e_u \\ &= (I + PC_{fb})^{-1} r_d \end{aligned} \tag{11}$$

The term $(\boldsymbol{I}+\boldsymbol{PC}_{fb})^{-1}$ exists since both $\boldsymbol{P}$ and $\boldsymbol{C}$ are diagonal matrices with nonzero elements. Then, the formulation for the uncoupled contour error, ε_u, can be obtained as shown in (12).

$$\varepsilon_u = C^T e_u = C^T (I + PC_{fb})^{-1} r_d \tag{12}$$

To calculate the coupled contour error, ε, first the coupled axial error, e, (i.e., $C_{cc} \neq 0$) is found as shown in (13).Then this error is multiplied by the coupling gains as given in (14).

$$\begin{aligned} e &= r_d - r \\ &= r_d - P(C_{fb}e + CC_{cc}C^T e) \\ &= (I + PC_{fb} + PCC_{cc}C^T)^{-1} r_d \end{aligned} \tag{13}$$

$$\varepsilon = C^T e = C^T (I + PC_{fb} + PCC_{cc}C^T)^{-1} r_d \tag{14}$$

CETF, H, is defined as the relationship between uncoupled and coupled systems as shown in (15).

$$\varepsilon = H\varepsilon_u \tag{15}$$

Using (12), (15) can be written as

$$H\varepsilon_u = HC^T (I + PC_{fb})^{-1} r_d \tag{16}$$

Then, using (14) and (16), (17) can be obtained.

$$C^T ((I + PC_{fb}) + PCC_{cc}C^T)^{-1} = HC^T (I + PC_{fb})^{-1} \tag{17}$$

By using the matrix inversion lemma

$$\begin{aligned} &C^T ((I + PC_{fb}) + PCC_{cc}C^T)^{-1} = \\ &\quad C^T (I + (I + PC_{fb})^{-1} PCC_{cc}C^T)^{-1} (I + PC_{fb})^{-1} \end{aligned} \tag{18}$$

Equations can further be simplified to find H as in (21):

$$C^T (I + (I + PC_{fb})^{-1} PCC_{cc}C^T)^{-1} = HC^T \tag{19}$$

$$C^T = H(C^T + C^T (I + PC_{fb})^{-1} PCC_{cc}C^T) \tag{20}$$

$$H = (I + C^T (I + PC_{fb})^{-1} PCC_{cc})^{-1} \tag{21}$$

Since H is a transfer function with one dimension (21) can be re-written as

$$H = \frac{1}{1 + C^T (I + PC_{fb})^{-1} PCC_{cc}} = \frac{1}{1 + P_e C_{cc}}, \tag{22}$$

where $P_e = \boldsymbol{C}^T(\boldsymbol{I}+\boldsymbol{PC}_{fb})^{-1}\boldsymbol{PC}$ can be considered as an equivalent controlled plant. The gain values in C change between -1 and 1 throughout the motion. Therefore, the equivalent controlled plant has varying parameters. Although these gains change during the motion, they do not vary between iterations because they are used for the same reference contour. Since the CETF, H, can be considered as the sensitivity function of the (C_{cc}, P_e) system as shown in (22), the cross-coupled controller can be designed using conventional robust single-input-single-output control methods. Therefore, a stabilizing controller C_{cc} can be

designed for this system using traditional feedback stability and robustness techniques after each single-axis loop is designed to be stable. Moreover, according to the theorem given in [25], the cross-coupled system is internally stable if the single-axis feedback controllers achieve internal stability for each axis and the cross-coupled controller keeps the equivalent control system (C_{cc}, P_e) internally stable while the coupling gains vary.

Convergence of the ILC via zero phase filtering on a cross-coupled system can be shown by extending the convergence analysis for the single-axis system given in [9] or other researchers such as [26]. For the convergence analysis, some assumptions should be made. Firstly, single-axis plants and the cross-coupled control system should internally stable. Furthermore, the number of inputs should be equal to the number outputs in the system. There should be a unique desired input $\boldsymbol{u}^d$ for a desired trajectory $\boldsymbol{r}_d$. Considering control signals as an indication of plant dynamics, $\boldsymbol{u}_i$ can be separated into its repeatable and non-repeatable components as $\boldsymbol{u}_R{}^d$ and $\boldsymbol{u}_{NR}{}^i$ (i.e., $\boldsymbol{u}^i$=$\boldsymbol{u}_R{}^d$+$\boldsymbol{u}_{NR}{}^i$), respectively where the non-repeatable part is bounded by $\boldsymbol{h}_m$'*$\boldsymbol{u}_{NR}{}^i \leq \varepsilon^*$ for $\forall i$ where * is the convolution operator.

If the given assumptions are satisfied and the task is performed repeatedly, $\boldsymbol{u}_{ff}{}^i$ approaches $\boldsymbol{u}_R{}^d$ as i increases when $\varepsilon^* \rightarrow 0$. In real applications, ε^* is small and can be assumed as 0. Therefore, as ε^* goes to zero (23) is satisfied.

$$\mathbf{u_i} = \mathbf{u_R^d} + \mathbf{u_{NR}^i} \tag{23}$$

In the proposed control structure, ILC via zero phase filtering is used for all single-axis loops. Since each axis tracking is convergent, the contour error is also convergent. Convergence analysis for simulations and experiments are performed for the trajectories given in Section V. Convergence of the RMS (root mean square) contour error is shown in Fig. 9 for both simulation and experiment. In Part (a) of Fig. 9 RMS contour error for simulations converges to a value which is very close to zero. For the experiments (Fig. 9 (b)), convergence is not as smooth as the simulations due to unrepeated disturbances and nonlinearities. The RMS contour error converges to a value around *30nm*. Convergence to *30nm* RMS contour error value can be considered as an acceptable result since the encoder resolution used for the experiments is *25nm*.

5. SIMULATION RESULTS

To investigate the performance of the two-axis positioning system a detailed simulation analysis is done. In the simulations, velocity profiling approach has been used to generate individual axis reference trajectories. A generic *S*-curve method is employed for this purpose. The two-axis positioning system is simulated with a nonlinear contour as the desired input. The cross coupling gains (i.e. $C_i s$), are equal to the normal vector elements of the contour. For comparison of the performances the plant model is simulated with feedback control only (FB), feedback control with cross-coupled control (FB CCC), feedback control with iterative learning control (FB ILC) and feedback control with cross-coupled control and iterative learning control with zero phase filter (FB CCC ILC). The performance of all of these control schemes are summarized in Table 2. In the table, root mean square (RMS) of the error signals has been used. As expected from our earlier derivations the worst positioning performance of the system is obtained when only the feedback controller is used. Then, the axis performance is improved drastically when the ILC is introduced. As the last addition, it can be observed that combining ILC and CCC with FB (i.e., our method) gives the best results as expected. This combination benefits from both tracking performance improvements of using ILC and contouring performance improvements of using CCC.

The nonlinear contour used in simulations is given in Fig. 10(a) at the top portion of the plot. In the figure, the zoomed view is taken from the part with a turn that is shown with the box on the original contour because contour tracking is more challenging during turns. The figure shows contouring performance of the system for the nonlinear contour is improved significantly when the proposed method (FB CCC ILC) is used instead of only the feedback (FB) control.

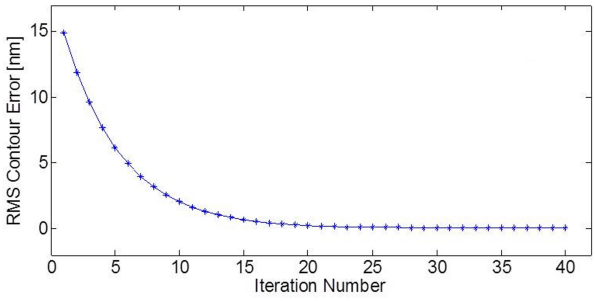

(a)

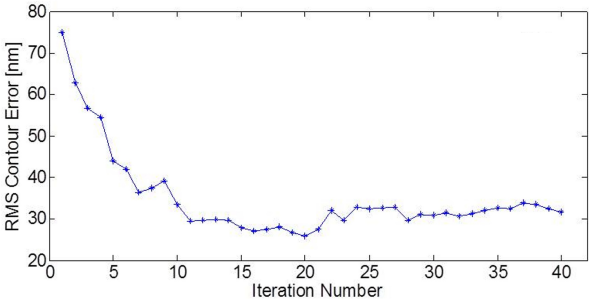

(b)

Fig. 9. RMS contour error for (a) simulation and (b) experiment.

Table 2. Two-axis System simulation - RMS error values

RMS Error	x-axis	y-axis	contour
FB	11.30	111.27	29.04
FB CCC	15.42	110.65	32.36
FB ILC	3.47	2.17	2.73
FB CCC ILC	1.09	2.11	0.78

6. EXPERIMENTAL RESULTS

For the system shown in Fig. 1 and Fig. 2 an experimental study was conducted to see the real life performance of the system with the proposed control approach. In order to validate our position measurements externally, a test setup is prepared using a two-arm differential laser vibrometer with *3nm* measurement resolution. One of the laser arms is directed to the stationary part of the slider as the reference and the other arm is positioned to point at the moving part of the slider system as shown in Fig.11. The same contour with the same velocity profile, which is used for simulations, is also used for the experiments. The contour tracking of the two-axis system with only feedback (FB) control and feedback control with CCC and ILC with zero phase filter (FB CCC ILC) is given in Fig. 10. The figure shows proposed control design improved contouring performance considerably. When Parts (a) and (b) of Fig. 10 is compared, simulations and experiments present a similar behavior such as deteriorated contour control just after the turn. FB CCC ILC system gives better contouring result than FB only in both cases. Due to the unmodelled dynamics and disturbances in the experiment setup, FB CCC ILC design does not improve the contouring performance as much as it does in the simulations.

In order to compare the experimental results with the simulation work presented in the previous subsection, further experiments conducted with using feedback control (FB), feedback control with cross-coupled control (FB CCC), feedback control with iterative learning control (FB ILC) and feedback control with cross-coupled control and iterative learning control (FB CCC ILC). Variation of RMS single-axis errors and RMS contour error with the different control schemes are given in Table 3. From Table 3, it can be observed that FB CCC system decreases contour error significantly as well as improvements in axial errors. Similarly, FB ILC system decreases axial tracking errors more effectively than contour error as expected. Best tracking and contouring performance is obtained for FB CCC ILC system as for the simulation case. All axial tracking errors and the contour error is improved approximately by *50%* as compared to the case where only feedback control is used.

7. CONCLUSION

In this paper, a new method that combines cross-coupled control and iterative learning control approaches

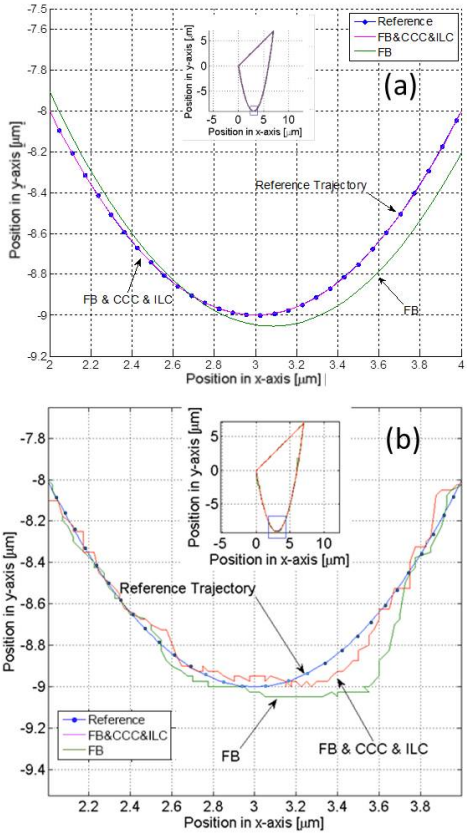

Fig. 10. (a) Simulation and (b) experimental results of two-axis system for the nonlinear contour.

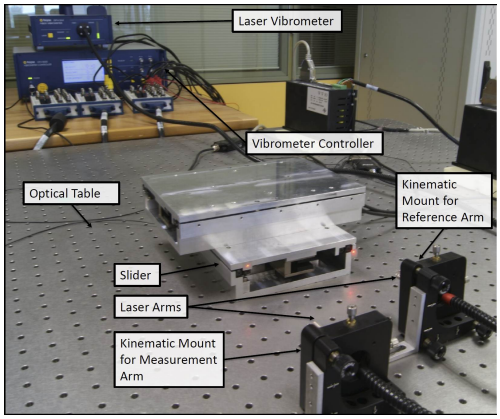

Fig. 11. External validation of axis position data.

Table 3. Two-axis system experiments - RMS error values

RMS Error	x-axis	y-axis	contour
FB	46.84	113.05	57.08
FB CCC	42.06	94.66	43.49
FB ILC	25.81	79.14	39.33
FB CCC ILC	21.28	66.69	27.52

which improves the contour and the tracking accuracy of the positioning systems at the same time is presented. Improving tracking accuracy

generally increases the contour performance except for the cases where the system dynamics interactions and friction effects dominate. Our method is computationally more efficient, more suitable for coupling gain calculations of arbitrary nonlinear contour and easier to implement on multi-axis positioning systems with increased mechatronic modularity. This stage system is modular in the sense that multiple identical stages can be assembled together to form positioning systems without changing the stage control algorithm (i.e., mechatronic modularity). The increased modularity of the system compared to similar solutions is important since it improves desired lifecycle properties such as maintainability, upgradability, diagnosability of a system. Stability and convergence analysis of the proposed controller is provided. Tracking and contouring performance of the method on a nonlinear contour is verified through simulations and experiments. The controller achieves nanometer level accuracy for the two-axis system. In the experiments, RMS error of x-axis, RMS error of y-axis and RMS contour error of the two-axis system is decreased to *21nm*, *66nm* and *27nm* respectively. This result is substantial improvement over using only a feedback controller for each stage which results in error values of *46.84nm*, *113.05nm* and *57.08nm* respectively. As future work the proposed multi-axis controller will be implemented on a three-axis system and axis controller will be improved.

REFERENCES

[1] R. Seifabadi, S. M. Rezaei, S. S. Ghidary, and M. Zareinejad, "A teleoperation system for micro positioning with haptic feedback," *International Journal of Control, Automation and Systems* , vol. 11, no. 4, pp. 768–775, Aug. 2013.

[2]]L. Lihua, L. Yingehun, G. Yongfeng, and S. Akira,"Design and testing of nanometer positioning system," *Journal of Dynamic Systems, Measurement and Control*, vol. 132, no. 2, pp. 021011–6, 2010.

[3] S. M. Raafat, R. Akmeliawati, and W. Martono, "Intelligent robust control design of a precise positioning system," *International Journal of Control, Automation and Systems*, vol. 8, no. 5, pp. 1123–1132, Oct. 2010.

[4] M. Tomizuka, "Zero phase error tracking algorithm for digital control," *Journal of Dynamic Systems, Measurement and Control*, vol. 109, no. 1, pp. 65–68, 1987.

[5] P. Hsu, Y. Houng, and S. Yeh, "Design of an optimal unknown unknown input observer for load compensation in motion systems," *Asian Journal of Control*, vol. 3, no. 3, pp. 204–215, 2001.

[6] L. Qing, W. Tai-yong, D. Ying-chuan, J. Yong-xiang, and L. Bo, "Applications of position controller for cnc machines based on state observer and cross-coupled controller," *Proc. of International Conference on Computer Mechatronics, Control and Electronic Engineering (CMCE)*, pp. 593–596, 2010.

[7] M. Tomizuka, "Friction compensator for feed drive systems consisting of ball screw and linear ball guide," *Proc. of the 35th International MATADOR Conference*, pp. 311–314, 2007.

[8] L. Wang, S. Lin, and H. Zeng, "Precision contour control of XY table based on LuGre model friction compensation," *Proc. of 2nd International Conference on Intelligent Control and Information Processing (ICI-CIP)*, pp. 1124–1128, 2011.

[9] K. K. Tan, H. Dou, Y. Chen, and T. H. Lee, "High precision linear motor control via relay-tuning and iterative learning based on zero-phase filtering," *IEEE Transactions on Control Systems Technology* , vol. 9, no. 2, pp. 244–253, 2001.

[10] K. L. Barton and A. G. Alleyne, "A cross-coupled iterative learning control design for precision motion control," *IEEE Transactions on Control System Technology*, vol. 16, no. 6, pp. 1218–1231, 2008.

[11] G. Pipeleers and K. L. Moore, "Reduced-Order Iterative Learning Control and a Design Strategy for Optimal Performance Tradeoffs," *IEEE Transactions on Automatic Control*, vol. 57, no. 9, pp. 2390–2395, Sep. 2012.

[12] Z. R. Novakovic, *The Principle of Self Support in Control Systems* Amsterdam, Elsevier, Netherlands, vol. 8, 1992.

[13] H. S. Ahn, Y. Q. Chen, and K. L. Moore, "Iterative learning control: Brief summary and categorization," *IEEE Transactions on Systems, Man, and Cybernetics, Part C: Applications and Reviews*, vol. 37,no. 6, pp. 1099–1121, 2007.

[14] Y. Koren and C. C. Lo, "Variable gain cross-coupling controller for contouring," *CIRP Annals Manufacturing Technology* , vol. 40, no. 1, pp. 371–374, 1991.

[15] L. Tang and R. G. Landers, "Multiaxis contour control the state of the art," *IEEE Transactions on Control Systems Technology*, vol. 21, no. 6, pp. 1997–2010, Nov. 2013.

[16] Y. Koren, "Cross-coupled biaxial computer control for manufacturing systems," *Journal of Dynamic Systems, Measurement and Control* , vol. 102, no. 4, pp. 265–272, 1980.

[17] M. Naumovic and M. Stojic, "Design of the observer based cross-coupled positioning servo drives," *Proc. of the IEEE International Symposium on Industrial Electronics, ISIE '97*, vol. 2, 1997.

[18] H. Y. Chuang and C. H. Liu, "A model referenced adaptive control strategy for improving contour accuracy of multi-axis machine tools," *Proc. of the 1990 IEEE Industry Applications Society Annual Meeting*, 2, Ed., pp. 1539–1544, 1990.

[19] K. L. Barton and A. G. Alleyne, "Cross-coupled ilc for improved precision motion control: design and implementation," *Proc. of the American Control Conference*, pp. 5496–5502, 2007.

[20] H. S. Li, X. Zhou, and Y. Chen, "Iterative learning control for cross-coupled contour motion systems," *Proc. of IEEE International Conference Mechatronics and Automation,*, vol. 3, pp. 1468–1472, 2005.

[21] S. S. Yeh and P. L. Hsu, "Estimation of contouring error vector for the cross-coupled control design," *IEEE/ASME Transaction on Mechatronics* , vol. 7, no. 1, pp. 44–51, 2002.

[22] N. Gecer-Ulu, E. Ulu, and M. Cakmakci, "Learning based cross-coupled control for multi-axis high precision positioning systems," *Proc. ASME Dynamic Systems and Control Conf. (DSCC 2012)* , Ft. Lauderdale, FL, Oct 2012.

[23] E. Ulu, N. Gecer Ulu, and M. Cakmakci, "Development and Validation of an Adaptive Method to Generate High-Resolution Quadrature Encoder Signals," *Journal of Dynamic Systems, Measurement, and Control*, vol. 136, no. 3, May 2014.

[24] K. Ogata, *Modern Control Engineering*, Prentice Hall, 1990.

[25] S. S. Yeh and P. L. Hsu, "Theory and applications of the robust cross-coupled control design," *Proc. of the American Control Conference*, pp. 791–795, 1997.

[26] T. Y. Doh, J. R. Ryoo, and D. E. Chang, "Robust iterative learning controller design using the performance weighting function of feedback control systems," *International Journal of Control, Automation and Systems*, vol *12, no.* 1, pp.63-70, 2014.

Nurcan Gecer-Ulu is a graduate student in Mechanical Engineering at Bilkent University in Ankara, Turkey. She received her B.S degree in Mechanical Engineering from M.E.T.U Ankara in 2010. Her research areas include modeling, analysis and control of dynamic systems and smart mechatronics.

Erva Ulu is a graduate student in Mechanical Engineering at Bilkent University in Ankara, Turkey. He received his B.S degree in Mechanical Engineering from M.E.T.U Ankara in 2010. His research areas include mechatronic design, modeling, analysis and control of dynamic systems.

Melih Cakmakci is an Assistant Professor of Mechanical Engineering at Bilkent University in Ankara, Turkey. He received his B.S degree in Mechanical Engineering from M.E.T.U Ankara in 1997. He received his M.S and Ph.D. in Mechanical Engineering Degrees from University of Michigan in 1999 and 2009 respectively. His research areas include modeling, analysis and control of dynamic systems, Prior to joining Bilkent University, he was a senior engineer at the Ford Scientific Research Center. He is a member of ASME, IEEE and SAE.